Modifying the high-energy part of the above-threshold-ionization spectrum

I. A. Ivanov*

Research School of Physical Sciences and Engineering, The Australian National University, Canberra ACT 0200, Australia

(Received 27 June 2010; published 8 September 2010)

We show that the high-energy part of the above-threshold-ionization spectrum can be modified considerably if a driving laser pulse composed of several harmonic frequencies is used. To find such a pulse we rely on classical calculation. We present results of the quantum-mechanical calculation confirming classical results.

DOI: 10.1103/PhysRevA.82.033404 PACS number(s): 32.80.Fb, 42.65.Ky

I. INTRODUCTION

Processes of above-threshold ionization (ATI) [1] and high harmonic generation (HHG) [2,3] occur for atoms interacting with long-wavelength high-intensity laser pulses. An appealing feature of both phenomena is that their essential features can be understood using the following well-known classical model [1,2,4,5].

First, at some moment of time t_0 atomic ionization event occurs. As a result, the electron emerges into the continuum with zero velocity. This event defines initial conditions for the subsequent electron motion which in this model is considered entirely classical. For some moments of time t_0 the electron can eventually return to the nucleus. The electron can then either recombine emitting a photon, or rescatter and acquire subsequently yet more energy from the laser field. The first possibility gives us a classical description of the HHG process; the second provides an explanation of the appearance of high-energy electrons in the ATI spectrum. This classical model predicts that electron kinetic energy at the moment of return to the nucleus cannot exceed the value of approximately $3.2U_p$. If the rescattering event occurs, the classical model gives another bound for the maximum kinetic energy the electron can acquire—$10U_p$. Here, $U_p = F_0^2/4\omega^2-$ ponderomotive potential, and F_0 and $\omega-$ are the amplitude and frequency of the driving electromagnetic (EM) field. These bounds give the well-known cutoff rules for ATI and HHG spectra, giving correspondingly the maximum photon energy which the recombination event can produce if the HHG scenario occurs, or the maximum electron energy in the ATI spectrum if the electron rescatters. Existence of these cutoffs has been demonstrated by quantum-mechanical calculations [3,6,7].

Success of the classical model in reproducing essential features of these phenomena can be related to the fact that for the field parameters typically considered, electron motion is essentially semiclassical [3,8]. That gives us reason to believe that the classical calculation outlined previously can be used as a reliable guide for the solution of the problems, which otherwise would be quite challenging computationally. We may, for example, inquire which particular pulse shape can be used to increase the cutoffs values for the HHG or ATI processes. Of course, for such a problem to make sense, we must impose some constraints, such as the requirement that the solution is sought for the pulses carrying a given fixed amount of energy.

Such questions belong to the field of the quantum optimal control theory [9]. Solution of such problems using purely quantum mechanical methods, such as the genetic algorithm [10], or variational formulation of the time-dependent Schrödinger equation (TDSE) and the constraints [9], demand multiple solutions of the TDSE. This may present a considerable computational burden if one is interested in applications to real atomic systems, and no approximations, such as reducing the problem to a one-dimensional one, are made.

We may use the previously mentioned fact of considerable predictive power of the classical model to facilitate this task. The classical model described above can easily be applied for any pulse shape of the driving EM field as was done, for example, in [11], or will be done in the following. The classical calculation must, of course, be supplemented with the quantum-mechanical calculation to verify that the desired goal, such as extension of the cutoff value, has indeed been achieved. We cannot accept the results of the classical calculation completely unreservedly since the classical model described above neglects the effect of the atomic potential on the electron motion.

For the HHG process, such a program has been realized in Refs. [12,13] and in our recent paper [14]. In Ref. [12] a classical wave form was found allowing one to maximize the classical cutoff value for the HHG process in the class of wave forms which are periodic with a given period $T = 2\pi/\Omega$. Such a wave form was found to contain a dc component. If the presence of dc component in the pulse is not desirable, it was shown [13] that the effect of the dc component can to some extent be mimicked by including the subharmonic ac field of $\Omega/2$ frequency. Adding such subharmonic components to the pulse allows one to increase the HHG cutoff value considerably. Classical results were confirmed in these works by the quantum-mechanical calculation. In our paper [14] we restricted the class of the possible wave forms to the wave forms which are periodic with a period $T = 2\pi/\Omega$ and do not contain the subharmonic frequencies. In this case, as the classical calculation presented in our paper shows, increase of the HHG cutoff value is also possible. Results of the quantum-mechanical calculation taking into account the effect of the atomic potential, which we presented in that work, confirm the classical result.

In the present work we apply this strategy for the ATI process. We shall look for the pulse shape among a certain class of the pulse shapes for which classical calculation yields the maximum possible increase of the classical cutoff value for the ATI spectrum. We shall present results of an *ab initio* calculation of the ATI spectrum for the laser pulse having this shape. We shall see that considerable increase in the spectral

*Igor.Ivanov@.anu.edu.au

intensity in the region of high electron energies can be achieved using such a laser pulse.

II. THEORY

In this section we consider motion of an electron driven by the laser pulse of the following form:

$$F(t) = 2f(t)\mathrm{Re}\sum_{k=1}^{K} a_k e^{ik\Omega t}, \tag{1}$$

where envelope function is chosen to be $f(t) = \sin^2 \frac{\pi t}{T_1}$, $T_1 = 10T$ is total duration of the pulse, and $T = 2\pi/\Omega$ is an optical cycle corresponding to the frequency Ω. Summation in Eq. (1) starts with $k = 1$ which ensures that the EM field given by this equation does not contain a dc component. Field is assumed to be linearly polarized along the z axis.

We shall be interested below in finding the set of the coefficients a_k describing the field, for which the ATI spectrum can be extended beyond the cutoff value of $10U_p$ as far as possible. Obviously, for this problem to be legitimately posed, we have to impose restrictions on the possible choices of the coefficients a_k. We shall consider only the pulses which carry a given fixed amount of energy, that is, we impose the restriction $\int_0^{T_1} F^2(t)\,dt = \int_0^{T_1} \mathcal{E}^2(t)\,dt$. Here $\mathcal{E}(\sqcup)$ is a "standard" pulse $\mathcal{E}(t) = \mathcal{E}_0 f(t)\cos\Omega t$, where $f(t)$ is the same envelope function as in Eq. (1). The "standard" pulse $\mathcal{E}(t)$ is obtained if we put $a_1 = \mathcal{E}_0/2$ and $a_k = 0$ for $k > 1$ in Eq. (1). We chose parameters of the "standard" pulse as follows. The peak strength was chosen to be $\mathcal{E}_0 = 0.1068$ a.u., corresponding to the peak intensity of 4×10^{14} W/cm^2, the base frequency was $\Omega = 0.114$ a.u, corresponding to the wavelength of 390 nm. We have to retain only a reasonably small number of harmonic frequencies in Eq. (1). The calculation described below shows that the increase in photoelectron energies, which can be achieved by adjusting parameters a_k, reaches a plateau rapidly when K exceeds the value $K = 5$; choosing larger values for this parameter produces no appreciable effect. We shall, therefore, use the value $K = 5$ for the permissible pulse shapes in all calculations in the following.

The problem we shall tackle can thus be reformulated as follows. Find the set of the coefficient a_k in Eq. (1) for which the ATI cutoff value obtained classically attains a maximum, provided that total energy carried by the pulse is the same as that of the "standard" pulse of the central wavelength 390 nm and 4×10^{14} W/cm^2 peak intensity. In the next section we give a solution to this problem using purely classical analysis of the electron trajectories. For brevity, we shall call below the pulse characterized by this set of a_k's the "maximum" pulse.

To confirm, for the pulse thus found, that the ATI spectrum does extend beyond the cutoff value of $10U_p$, we will subsequently perform a quantum-mechanical calculation of the ATI spectra for the "standard" and "maximum" pulses for the hydrogen atom.

A. Classical calculation

We shall follow below the standard classical treatment of the ATI process described in [4,11]. This treatment is based on the analysis of the classical trajectory which originates at some moment of time t_0 in the interval $(0,T_1)$ of the duration of the pulse, and for which electron returns to the nucleus at some later time t_1. For the purpose of determination of the maximum kinetic energy of photoelectrons it is sufficient to consider classical motion only along the z coordinate, which is assumed to be the direction of the pulse polarization. Also, as the standard classical model prescribes, we neglect any influence of the atomic potential on the electron motion, considering only the effect of the laser field.

Initial conditions for classical equations of motion for each such trajectory are $z = 0$, $v = 0$. Let the velocity of an electron at the moment t_1 of return to the nucleus be v_1. An electron can acquire maximum kinetic energy if a backscattering event occurs. The velocity of an electron then becomes $-v_1$, and for the final velocity which the electron acquires after the end of the pulse, one may write [4,11] $v_{\mathrm{fin}} - A_{\mathrm{fin}} = -v_1 - A(t_1)$, where $A(t_1)$ is the value of the vector potential at the moment t_1, A_{fin} is the value of the vector potential after the end of the pulse. The latter statement is a consequence of the fact that combination $v - A$ is a canonical momentum and is an integral of motion if the atomic potential is neglected. If the vector potential is calibrated so (as in the present work) that its value after the end of the pulse is zero, then for the final velocity of the electron one gets $v_{\mathrm{fin}} = -v_1 - A(t_1)$. We can thus determine the kinetic energy which the electron possesses after the end of the pulse.

We can perform this procedure for any set of the coefficients a_k in Eq. (1). For each set of a_k's we consider all returning trajectories originating at various times t_0 inside the interval $(0,T_1)$ of the duration of the pulse. For a trajectory originating at a given moment of time there may be several subsequent return events in the interval $(0,T_1)$. Among those we choose that for which final kinetic energy is the largest. This gives us final kinetic energy $E(t_0,\boldsymbol{a})$ as a function of the moment of time t_0 when the ionization event occurs, and a set of coefficients a_k. For a given set of a_k's we seek a maximum of $E(t_0,\boldsymbol{a})$ with respect to t_0- time when ionization occurs. The resulting quantity is a function of the set of a_k's only. We now maximize this quantity in the five-dimensional complex space of the coefficients a_k, imposing the restriction of the constant total energy carried by the pulse.

This strategy gives us the set of coefficients a_k listed in Table I.

These pulses can be visualized with the help of Fig. 1, where central parts of both "standard" and "maximum" pulses are shown.

TABLE I. Coefficients in Eq. (1) for the "standard" pulse and for the pulse for which the classical ATI cutoff attains the largest value ("maximum" pulse). Second column shows the "standard" pulse; third column is the "maximum" pulse.

k	Standard pulse $a_k \times 10^2$	Maximum pulse $a_k \times 10^2$
1	5.34	$4.672 + 0.262i$
2	0	$0.356 - 1.979i$
3	0	$-1.017 - 0.023i$
4	0	$-0.543 + 0.645i$
5	0	$0.654 + 0.588i$

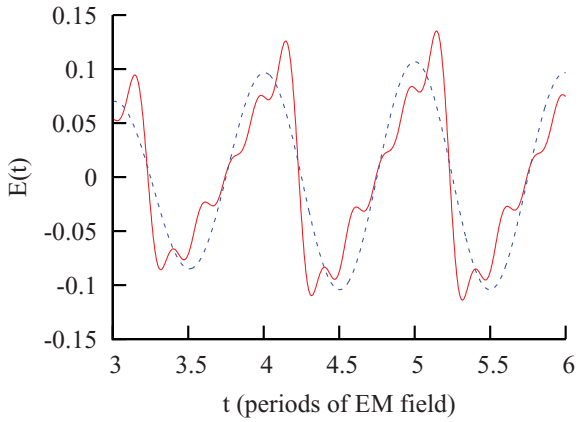

FIG. 1. (Color online) EM field for the "standard" pulse (blue) dashed line, and "maximum" pulse (red) solid line.

Figure 2 illustrates the classical calculation we described above for "standard" and "maximum" pulses.

In Fig. 2 we plot the quantity $E(t_0,\boldsymbol{a})$ we introduced previously—the largest final kinetic electron energy for all classical trajectories starting at the moment of time t_0 for two sets of a_k's from Table I, corresponding to the "standard" and "maximum" pulses. Figure 2 shows the ratio of the kinetic energy and the ponderomotive potential, defined as $U_p = \mathcal{E}_0^2/(4\omega^2)$, where $\mathcal{E}_0 = 0.1068$ a.u. is the peak strength of the "standard" pulse.

One can see that the "standard" pulse maximum kinetic energy, which the electron can attain, is approximately $10U_p$. This is, of course, a visualization of the well-known classical cutoff rule. For the "maximum" pulse the energy of approximately $13.5U_p$ can be attained. In both cases, the maxima are attained for the trajectories starting near the center of the pulse. This is, of course, to be expected, since it is there the EM field attains the peak strength. Interestingly enough, for the "maximum" pulse, the trajectories starting as early as $3.5T$ can lead to the final maximum kinetic energies only slightly smaller than the trajectories starting near the middle of the pulse.

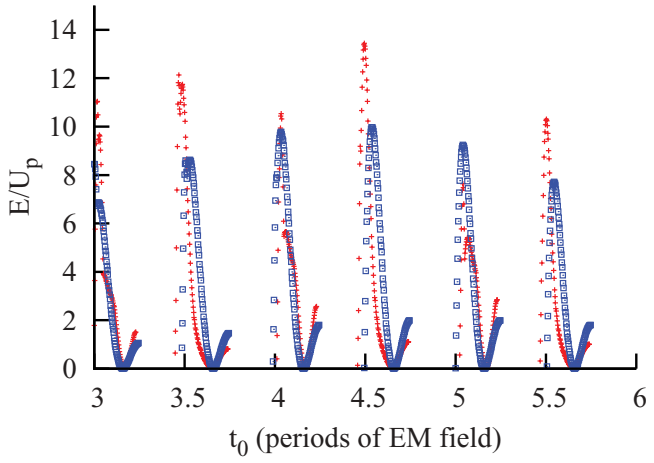

FIG. 2. (Color online) Classical dependence of the maximum final electron kinetic electron energy on the moment of time when the ionization event occurs. "Standard" pulse, (blue) boxes; "maximum" pulse, (red) crosses.

The foregoing discussion was based entirely on classical arguments, and neglected completely any effect of the atomic potential on the electron motion. Only the quantum-mechanical calculation, fully taking into account atomic structure, can confirm that the pulse obtained as described above indeed allows one to reach the desired goal of extension of the ATI spectrum beyond the classical cutoff value. Such calculation for the hydrogen atom is described in the next section.

B. Quantum-mechanical calculation

We seek a solution of the time-dependent Schrödinger equation for the hydrogen atom in the presence of the external EM field:

$$i\frac{\partial\Psi}{\partial t} = [\hat{H}_{\rm atom} + \hat{H}_{\rm int}(t)]\Psi, \tag{2}$$

where $\hat{H}_{\rm atom}$ is the Hamiltonian of the field-free atom, and operator $\hat{H}_{\rm int}(t)$ describes the interaction of the atom and the EM field. We use below the velocity form of this operator:

$$\hat{H}_{\rm int}(t) = \boldsymbol{A}(t)\cdot\hat{\boldsymbol{p}}. \tag{3}$$

Here, $\boldsymbol{A}(t) = -\int_0^t \boldsymbol{F}(\tau)\,d\tau$. The EM field $\boldsymbol{F}(t)$ is given by Eq. (1) with sets of coefficients a_k from Table I. We shall present below results of the calculations for both sets given in the table: the "standard" pulse and the "maximum" pulse.

We omitted the quadratic $\boldsymbol{A}^2(t)$ term in the interaction Hamiltonian (3). This term can always be removed through a gauge transformation [15], which amounts to multiplying the wave function by a phase factor. This is unimportant as long as we rely on the dipole approximation which is adopted in the present work.

We discretize the TDSE on a spatial grid with the step size $\delta r = 0.05$ a.u. using a box of the size $R_{\rm max} = 1700$ a.u. Temporal grid is equidistant; for each layer t_n the wave function is represented as

$$\Psi(\boldsymbol{r},t_n) = \sum_l f_l(r,t_n)Y_{l0}(\theta), \tag{4}$$

where functions $f_l(r,t_n)$ are defined in the points of the grid, and summation in Eq. (4) is restricted to $l = 0 - L_{\rm max}$; the particular value of this parameter will be specified below.

The Hamiltonian is discretized on the spatial grid using the three-point finite difference formulas for the second and first (for the interaction Hamiltonian) spatial derivatives. Transparent boundary conditions [16] are imposed on the functions f_l on the boundary of the box.

The choice of the gauge we use to describe atom-EM field interaction was dictated by the desire to keep the size of the expansion (4) relatively small. It is known [17,18] that for the two most commonly used gauges, length and velocity, expansion (4) exhibits very different convergence properties with respect to the number of the partial waves included. To achieve convergence with respect to the number of the partial waves in Eq. (4), a much smaller number of partial waves is needed if we use the velocity gauge. We used

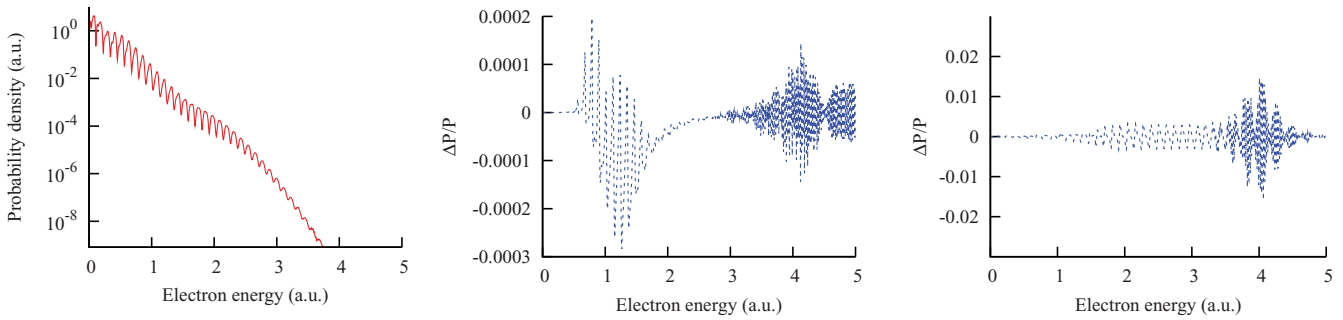

FIG. 3. (Color online) Electron spectrum $P(E)$ for $L_{\max} = 25$, $R_{\max} = 1700$ a.u. for the "standard" pulse from Table I (left panel). Relative error $[P(E) - P_1(E)]/P(E)$, where $P_1(E)$ has been computed with $L_{\max} = 20$, $R_{\max} = 1300$ (middle panel). Relative error $[P(E) - P_1(E)]/P(E)$, where $P_1(E)$ has been computed with $L_{\max} = 25$, $R_{\max} = 1700$ and time stepsize $\delta = 0.005$ a.u. (right panel).

$L_{\max} = 25$ in Eq. (4) for the calculations presented below. We will show below that this number is quite sufficient to obtain well-convergent results.

To propagate the wave function (4) in time we use the so-called matrix iteration method (MIM) developed in [18]. It has been shown [19] that this technique can be used for the efficient solution of the TDSE in strong EM fields.

The starting point for the development of the MIM procedure is the expression for the short-time Crank-Nicholson (CN) propagator [20]:

$$\Psi(\boldsymbol{r},t_n+\delta) = \frac{1 - i\hat{H}(t_n+\delta/2)\delta/2}{1 + i\hat{H}(t_n+\delta/2)\delta/2}\Psi(\boldsymbol{r},t_n). \tag{5}$$

The operator in the denominator in Eq. (5) can be partitioned as $1 + i\hat{H}(t_n+\delta/2)\delta/2 = \hat{A} + \hat{B}$, where $\hat{A} = 1 + i\hat{H}_{\rm atom}\delta/2$ and $\hat{B} = i\hat{H}_{\rm int}(t_n+\delta/2)\delta/2$.

Using the Neumann expansion for the $(\hat{A}+\hat{B})^{-1}$,

$$(\hat{A}+\hat{B})^{-1} = \hat{A}^{-1} - \hat{A}^{-1}\hat{B}\hat{A}^{-1} + \hat{A}^{-1}\hat{B}\hat{A}^{-1}\hat{B}\hat{A}^{-1}\ldots, \tag{6}$$

one reduces the problem of computing an inverse of the operator $1 + i\hat{H}(t_n+\delta/2)\delta/2$ in the expression for the CN short-time propagator to the repeated computation of the inverse of the operator $\hat{A}$ introduced previously.

For a function given by the expansion Eq. (4), where each $f_l(r,t_n)$ is represented on the spatial grid (r_n), this is a simple problem since $\hat{A}$ is diagonal in l and tridiagonal in n. Finding the inverse of $\hat{A}$ thus amounts to computing the inverse of a tridiagonal matrix, which can be done fast and efficiently. Convergence of the Neumann expansion (6) can be monitored choosing the time step size δ appropriately [18,19].

The electron spectrum $P(E)$ is obtained by projecting the solution of the TDSE at the end of the pulse on the set of the continuous spectrum wave functions of the hydrogen atom.

III. RESULTS

Before presenting results of the quantum-mechanical calculation described previously, we will discuss briefly issues related to the convergence of the calculation with respect to various parameters. We have performed several calculations varying parameters $L_{\max}$, $R_{\max}$, and time step size δ. As we mentioned previously, the results which we present as our final results have been obtained for $L_{\max} = 25$, $R_{\max} = 1700$ a.u. The time step size was $\delta = 0.0075$ a.u. and we retained the first six terms of the Neumann expansion (6).

On the left panel of Fig. 3 we present the electron spectrum $P(E)$ obtained for these values of the parameters for the "standard" pulse from Table I. The middle panel of the figure shows the relative error $(P(E) - P_1(E))/P(E)$, where $P_1(E)$ has been obtained using smaller values $L_{\max} = 20$, $R_{\max} = 1300$ a.u. in the calculation. Finally, on the right panel of the figure we show relative error $(P(E) - P_1(E))/P(E)$, where $P_1(E)$ has been obtained using $L_{\max} = 25$, $R_{\max} = 1700$ [the same as for $P(E)$] and a smaller time step size $\delta = 0.005$ a.u.

One can see that we have achieved very good convergence with respect to the number of partial waves and the box size. Relative error of the calculation when these parameters are varied does not exceed 3×10^{-4}. More restrictive is an error bound we obtain if we vary the time step size. We see that when time step size is reduced to 0.005 a.u. results for the most part of energy spectrum change by less than half of a percent except the energy region in the vicinity of $E = 4$ a.u., where results differ by approximately one percent. We can conservatively adopt the latter figure as an estimate of the accuracy of the calculation. The accuracy could be further improved by retaining a larger number of terms in the Neumann expansion, or reducing the time step size, but it is quite sufficient for the purpose of the present work.

In Fig. 4 we present results for electron spectra obtained for the "standard" and "maximum" pulses from Table I.

For the field parameters we use, the classical theory predicts for the "standard" pulse cutoff in the electron spectrum at energy of $10U_p \approx 2.5$ a.u. The quantum calculation shows that in agreement with the classical theory, spectral intensity indeed starts dropping fast for the energies exceeding this value. Again, in agreement with the classical predictions shown in Fig. 2, the electron spectrum for the "maximum" pulse extends into the region of higher energies. Spectral intensity in the case of the "maximum" pulse is indeed much higher for large electron energies, especially for the energies above the classical cutoff of 2.5 a.u. For the energies exceeding the classical cutoff the spectral intensity for the "standard" pulse drops sharply, and for the energies in the vicinity of 4 a.u. it is several orders of magnitude smaller than the intensity for the "maximum" pulse.

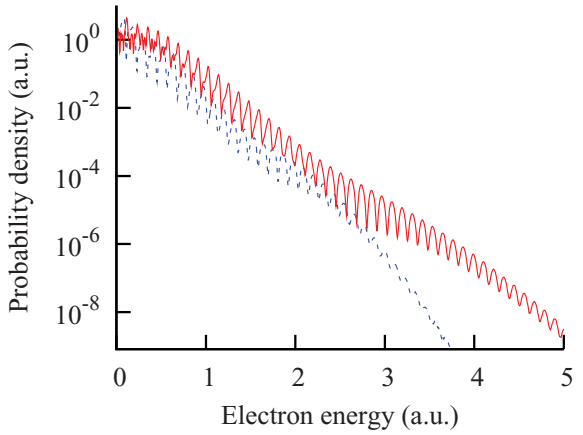

FIG. 4. (Color online) Electron spectra for the "maximum" [(red) solid line] and "standard" [(blue) dashed line] pulses.

The set of coefficients a_k characterizing the "maximum" pulse was found on the basis of a purely classical calculation neglecting any effect of the atomic potential on the electron motion. As we described previously, this set was obtained using the procedure which maximized the quantity $E(\boldsymbol{a})$—the highest kinetic energy which the electron may acquire upon leaving the field. In addition, fixed intensity constraint was imposed on the set of coefficients a_k. In other words, we searched for the maximum of $E(\boldsymbol{a})$ on the surface defined by the fixed intensity constraint in the space of the coefficients a_k. To find the maximum we used the gradient ascent method. For a given set of the starting values of a_k's this procedure converges to a local maximum of $E(\boldsymbol{a})$. The procedure was repeated many times with various sets of a_k's lying on the fixed intensity surface serving as starting values, until we were reasonably sure that the maximum we found was indeed the global maximum. In fact, the character (local or global) of this maximum is not very important for the following reasons.

We have found the maximum of the classically defined function $E(\boldsymbol{a})$. Figure 2 shows, that for the set of a_k's found in this way the spectral intensity of the high-energy part of the ATI spectrum also increases. To explain this fact, it will be convenient to give more precise meaning to the somewhat vague notion of the increase of the spectral intensity for high energies. We may, for example, introduce the function $I(\boldsymbol{a})$, defined as $I(\boldsymbol{a}) = \int_{10U_p}^{\infty} P(E)\, dE$. Here, $P(E)$ is the energy distribution which the quantum TDSE calculation gives for a laser pulse characterized by a given set of a_k's lying on the fixed intensity surface.

Figure 2 shows that increasing $E(\boldsymbol{a})$, we increase simultaneously $I(\boldsymbol{a})$. It is not guaranteed, of course, that at the point $\boldsymbol{a}$ on the fixed intensity surface, where $E(\boldsymbol{a})$ attains the global maximum, global (or even local) maximum of $I(\boldsymbol{a})$ is attained. What Fig. 2 demonstrates is that $I(\boldsymbol{a})$ shares with $E(\boldsymbol{a})$ some essential features, such as directions of growth. In the directions on the fixed intensity surface in which $E(\boldsymbol{a})$ grows, $I(\boldsymbol{a})$ can generally be expected to grow, though their maxima need not coincide. This is, of course, a consequence of the fact that the classical model neglecting effect of the atomic potential reproduces many features of the ATI phenomenon very well. We may expect that if we use a slightly more refined classical model e.g., the model taking into account the effect of the core potential on the electron motion) and repeat the same maximization procedure, we shall obtain another function $E_1(\boldsymbol{a})$, reproducing behavior of $I(\boldsymbol{a})$ on the fixed intensity surface even more closely. We may be able then to get yet closer to the true maximum of the function $I(\boldsymbol{a})$ on the fixed intensity surface.

We can easily include atomic potential in the classical calculation. Previously, we considered electron motion only in the direction of the EM field. For this one-dimensional problem Coulomb potential is too singular. We can, however, include in the calculation regularized Coulomb potential (the so-called soft-core potential), defined as $V(z) = -\frac{1}{\sqrt{z^2+b}}$, where we chose $b = 2.5$. This choice of the parameter b gives us the value of $10U_p$ for the classical cutoff energy in the case of the pure monochromatic driving field. With the core potential thus included in the classical equations of motion, the maximization procedure described previously was repeated.

The results are shown in Fig. 5. "Maximum" pulse on this figure is a pulse obtained using the maximization procedure with the soft-core Coulomb potential included in classical equations of motion.

A comparison of Fig. 5 and Fig. 4 shows, for the "maximum" pulse obtained if soft-core Coulomb potential is included in classical calculations, that the effect of the

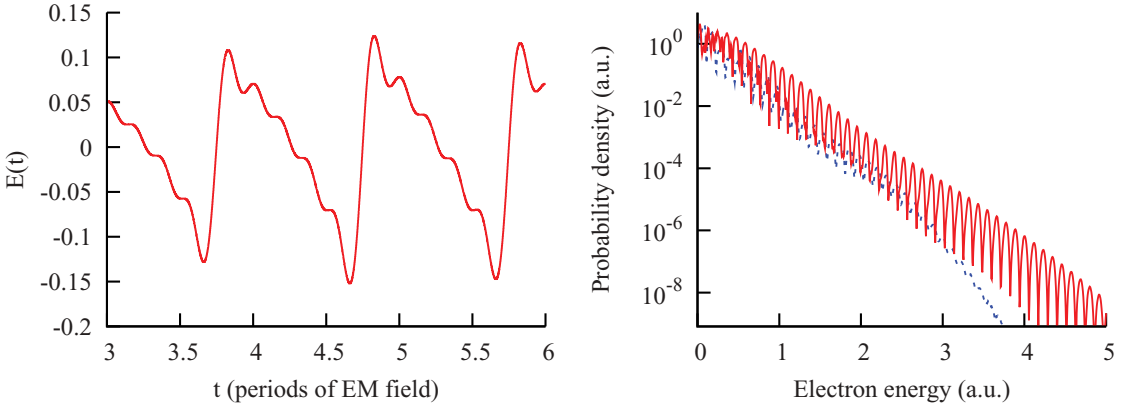

FIG. 5. (Color online) (Left) EM field for the "maximum" pulse obtained if the core potential is included in classical calculations. (Right) Electron spectra for the "maximum" [(red) solid line] and "standard" [(blue) dashed line] pulses.

extension of the ATI spectrum into the high-energy region is yet more pronounced than in the case of the "maximum" pulse shown in Fig. 4. We may explain this fact on the basis of the discussion presented previously. The function $E_1(\boldsymbol{a})$ obtained if we take into account the effect of the core potential on the electron motion probably reproduces essential features of $I(\boldsymbol{a})$, such as growth directions, better than the function $E(\boldsymbol{a})$. Therefore, at the point $\boldsymbol{a}$, where $E_1(\boldsymbol{a})$ attains a maximum on the fixed intensity surface we are closer to a local maximum of $I(\boldsymbol{a})$.

The local maxima of $I(\boldsymbol{a})$ which we approached with the help of the study of the extremum properties of functions $E(\boldsymbol{a})$ and $E_1(\boldsymbol{a})$, are probably two different local maxima. As a comparison of Figs. 1 and 5 (left) shows, "maximum" pulses are different in both cases.

The approach which we used brings us sufficiently close to a local maximum of $I(\boldsymbol{a})$, though not giving its exact position. Determination of the exact position of such a maximum, or search for the global maximum of this function constitutes, of course, a far more difficult and time-consuming task.

IV. CONCLUSION

We demonstrated that the ATI spectrum can be extended considerably into the high-energy region if we modify the driving pulse following prescriptions which the classical model provides. We saw that for the "maximum" pulse with the parameters summarized in Table I, which carries the same energy as the "standard" pulse, the spectral intensity for large electron energies (especially for energies above the classical cutoff) is indeed much higher.

The "space" of the permissible pulse shapes used to find the "maximum" pulse was given by Eq. (1), where we have put $K = 5$. Increasing the number of harmonic frequencies in this equation beyond this limit adds very little to the classical cutoff value, so the pulse shape with the coefficients from Table I provides the maximum cutoff value which can be achieved if we restrict the trial wave form to that given by Eq. (1) under condition of a fixed total energy carried by the pulse.

In finding the parameters of the "maximum" pulse we were governed by the purely classical notions, neglecting completely the effect of the atomic potential. As we have seen, results of the *ab initio* quantum TDSE calculation confirm the predictions of the classical theory. This is a gratifying feature of the present problem, which avoids using time-consuming techniques such as the genetic algorithm [10,21] requiring multiple solutions of the TDSE. We needed to include approximately 20 partial waves in the expansion (4) to achieve convergence. Repeating such a calculation many times would have been a rather serious computational challenge. Fortunately, the fact that classical model works so well saves us a lot of computing time.

Another goal we pursued in doing this work was testing the capabilities of the MIM method. It is known [18,19] that use of the MIM procedure and the velocity gauge for description of the atom-EM field interaction allows one to treat accurately the processes of multiphoton ionization in strong infrared fields, where a large number of photons can be absorbed from the laser field. We confirmed this fact for the EM fields described by Eq. (1), containing several harmonic frequencies.

ACKNOWLEDGMENTS

The author acknowledges support from the Australian Research Council in the form of the Discovery Grant (No. DP0771312). Resources of the National Computational Infrastructure (NCI) facility were employed.

[1] P. Agostini, F. Fabre, G. Mainfray, G. Petite, and N. K. Rahman, Phys. Rev. Lett. **42**, 1127 (1979).
[2] P. B. Corkum, Phys. Rev. Lett. **71**, 1994 (1993).
[3] M. Lewenstein, P. Balcou, M. Y. Ivanov, A. L'Huillier, and P. B. Corkum, Phys. Rev. A **49**, 2117 (1994).
[4] G. G. Paulus, W. Becker, W. Nicklich, and H. Walther, J. Phys. B **27**, L703 (1994).
[5] J. L. Krause, K. J. Schafer, and K. C. Kulander, Phys. Rev. A **45**, 4998 (1992).
[6] V. I. Usachenko and V. A. Pazderezsky, J. Phys. B **35**, 761 (2002).
[7] J. Wassaf, V. Véniard, R. Taïeb, and A. Maquet, Phys. Rev. A **67**, 053405 (2003).
[8] D. B. Milošević, J. Opt. Soc. Am. B **23**, 308 (2006).
[9] J. Werschnik and E. K. U. Gross, J. Phys. B **40**, R175 (2007).
[10] A. B. Yedder, C. Le Bris, O. Atabek, S. Chelkowski, and A. D. Bandrauk, Phys. Rev. A **69**, 041802(R) (2004).
[11] D. B. Milošević, G. G. Paulus, and W. Becker, Opt. Express **11**, 1418 (2003).
[12] S. B. P. Radnor, L. E. Chipperfield, P. Kinsler, and G. H. C. New, Phys. Rev. A **77**, 033806 (2008).
[13] L. E. Chipperfield, J. S. Robinson, J. W. G. Tisch, and J. P. Marangos, Phys. Rev. Lett. **102**, 063003 (2009).
[14] I. A. Ivanov and A. S. Kheifets, Phys. Rev. A **80**, 023809 (2009).
[15] R. Shakeshaft and X. Tang, Phys. Rev. A **36**, 3193 (1987).
[16] G. R. Hadley, Opt. Lett. **16**, 624 (1991).
[17] E. Cormier and P. Lambropoulos, J. Phys. B **29**, 1667 (1996).
[18] M. Nurhuda and F. H. M. Faisal, Phys. Rev. A **60**, 3125 (1999).
[19] A. N. Grum-Grzhimailo, B. Abeln, K. Bartschat, D. Weflen, and T. Urness, Phys. Rev. A **81**, 043408 (2010).
[20] A. Goldberg, H. M. Schey, and J. L. Scwartz, Am. J. Phys. **35**, 177 (1967).
[21] X. Chu and S.-I. Chu, Phys. Rev. A **64**, 021403(R) (2001).